Direct correlation of microtwin distribution with growth face morphology of CVD diamond films by a novel TEM technique

Z. L. Wang[a)]
Metals and Ceramics Division, Oak Ridge National Laboratory, P.O. Box 2008, Oak Ridge, Tennessee 37831-6376, and Department of Materials Science and Engineering, The University of Tennessee, Knoxville, Tennessee 37996

J. Bentley, R. E. Clausing, L. Heatherly, and L. L. Horton
Metals and Ceramics Division, Oak Ridge National Laboratory, P.O. Box 2008, Oak Ridge, Tennessee 37831-6376

(Received 15 December 1992; accepted 3 February 1994)

A thick as-grown diamond film was examined directly by conventional transmission electron microscopy (TEM) without thinning, and the important microstructures near the growth surface were characterized. Specimen preparation for TEM involved simply fracturing the film; some of the diamond grains located on the specimen edge were thin enough to be directly examined by TEM. The 3-D topography of the diamond grains located at the intersection of the growth and the fracture surfaces was obtained using secondary electron images, so that the 2-D projected grain geometry could be derived easily to help interpret the TEM images. A diamond film grown with a ⟨001⟩ texture and having grains 2–3 μm diameter with {001} facets parallel to the substrate and four inclined {111} facets was examined. Grains with fracture surfaces that intersected the top (001) facet, grains with fractures that intersected only {111} facets, and unfractured grains were studied. It was found that the core volume bounded by the (001) top facet and its projected column defined by orthogonal internal {110} were free from microtwins, but contained a few dislocations. The remaining volume around this core, bounded by {111} facets (or grain boundaries) and the internal {110}, was filled with microtwins. The microtwins were not merely at the {111} surfaces. Our results reveal a growth mechanism in which microtwins are formed as material is added to {111} but not {001}. The formation of microtwins in CVD diamond is thus clearly associated with growth on {111} surface facets.

I. INTRODUCTION

Diamond films grown by low pressure chemical vapor deposition (CVD) have many potential applications including optics and electronics. The quality of a diamond film is determined by the conditions under which the film was grown and is correlated with its surface morphology and internal microstructures. Scanning electron microscopy (SEM) is normally used to determine the size and shape distributions of diamond grains, but effectively provides only surface structural information. Microstructures within diamond grains can be directly imaged with the use of transmission electron microscopy (TEM), which can provide defect characterization at near atomic resolution.

In the TEM imaging technique, one of the most important steps is to prepare a thin specimen.[1–4] Since diamond is an extremely hard material, it is a tedious procedure to polish a diamond film to the thickness range appropriate for ion milling. The ion milling is also time consuming. Thus, specimen preparation greatly reduces the efficiency of applying TEM techniques for diamond studies. Conventionally, TEM information is from a thin internal section of material, and it can be difficult to deduce full 3-D structures needed to understand the growth mechanisms. Therefore, it is desirable to find new methods to prepare efficiently the diamond specimens for TEM and at the same time improve the correlation of internal microstructure with growth surface morphology.

To solve these problems, a novel TEM specimen preparation technique for diamond films is introduced in this paper. For the first time, an as-grown diamond film has been examined directly by conventional TEM without thinning, and the important microstructures near the growth surface have been characterized. The specimen preparation technique is introduced first, followed by its application to defect structures in a diamond film with a ⟨001⟩ texture. Finally, the growth mechanisms of the diamond films are discussed.

[a)]Send all correspondence to this author at current address, Metallurgy Division, NIST, Building 223, Room B106, Gaithersburg, Maryland 20899.

II. EXPERIMENTAL TECHNIQUES

As-grown diamond films were prepared for TEM examination in the following way. A diamond film (with or without silicon substrate) was fractured on a plane containing the growth direction. The fracture surface was usually irregular. For TEM examination, the film was loaded in a double-tilting holder and was tilted about 30–45° with respect to the TEM optic axis (see Fig. 1). With a SE (secondary electron) image for guidance, the microstructures of the diamond grains on the top edge of the growing face were examined using transmitted electron bright-field (BF) and dark-field (DF) TEM images and diffraction patterns. A diamond film with a 2 mm wide fractured edge contains hundreds of 2–3 μm grains on the fractured top edge. The analyses yielded common structural features of the entire film.

For this study, diamond films about 75 μm thick were grown with a hot filament system on a silicon (001) substrate at 930–935 °C in a mixture of H_2, CH_4, and CO gases. The as-grown film had a ⟨001⟩ texture. The surface morphology consisted of 2–3 μm-diameter grains, each with a (001) top facet surrounded by four inclined facets on {111}. Electron microscopy was performed with Philips CM30 (300 kV) and CM12 (120 kV) analytical electron microscopes (AEM's).

The topography of the film edge was determined by secondary electron (SE) imaging available in the same AEM. Since the secondary electrons image the specimen surface morphology, the 3-D geometrical shape of the grain can be easily identified. The 2-D projected geometry could be easily obtained to help interpret TEM images of the same grain. This is an important point that allows the defect distribution inside the grain volume to be exactly located with respect to the surface structure. Figures 2(a) and 2(b) show low-magnification SE images of a fractured diamond film recorded in the AEM. Figure 2(a), taken with the growth direction facing the SE detector, shows that the surface morphology consists of small grains with {001} and {111} facets. The topography of the fracture surface was clearly seen by tilting the specimen about 60° [Fig. 2(b)]. This type of image was very helpful for identification of the geometry of the newly formed fracture surface.

Only the grains that extend to the fracture edge of the film can be characterized to determine the relationship between the grain microstructures and the surface morphology. Figure 2(c) shows a low-magnification BF image of a fractured film in the geometry illustrated in Fig. 1. Diamond grains in different orientations are projected onto the same plane. It is possible to identify each individual grain and perform detailed TEM examinations.

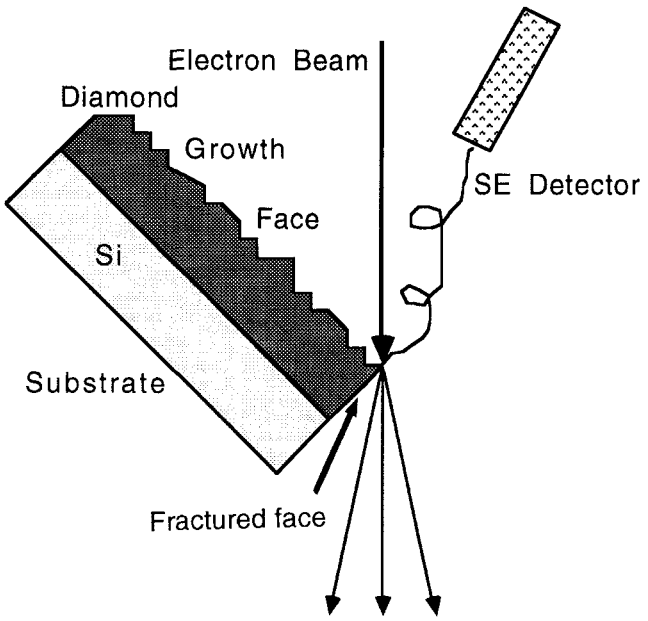

FIG. 1. A schematic diagram of specimen loading and imaging techniques for diamond studies with the "fracture" specimen preparation technique. The analytical electron microscope (AEM) is equipped with a secondary electron (SE) detector.

III. MICROSTRUCTURES OF DIAMOND FILMS

In general, it is difficult to construct an adequate 3-D structural model from a few TEM images that will allow the internal defect structure to be correlated with growth surface morphology. For example, for unfractured diamond grains, such as those shown in the SE image of Fig. 2(a), if the {111} facets surrounding the (001) top are covered with microtwins, the 2-D projected images along ⟨110⟩, ⟨112⟩, and ⟨113⟩ cannot provide accurate information as to whether the microtwins are located on the surface or inside the bulk. Images along (001) could indicate whether the microtwins are located near the grain boundary, but still cannot give the defect distribution inside the volume. This is a serious limitation on the application of TEM techniques for diamond studies.[1–4]

In our method, however, some of the grains located on the specimen edge are fractured transgranularly, so that one of the {111} facets and the material below it have been partly or totally removed by the fracture. This is the key fact that allows us to locate the defect distribution exactly. In the following sections, we report the studies of diamond grains fractured to allow examination of various parts of the interior of the diamond grains.

A. Grains with fracture surface intersecting top (001) facet

In many of the grains along the edge of the diamond film used in this investigation, the fracture surface

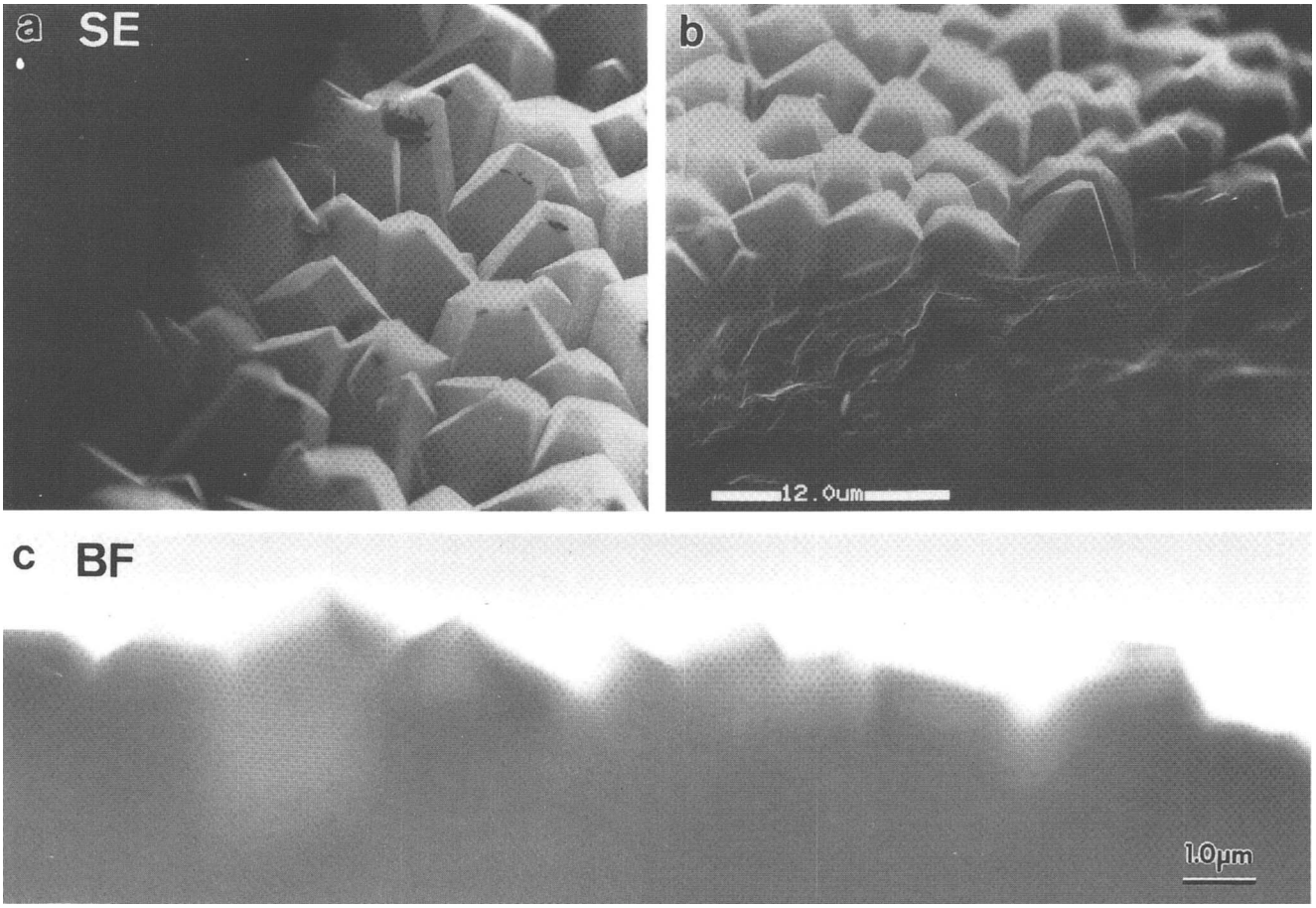

FIG. 2. Low magnification SE images of a fractured diamond film viewing from (a) close to film normal and (b) the fractured edge. Part (c) is a TEM image of the fractured film top edge in an AEM. The SE and TEM images can be complementarily used to define the microstructure and related surface features of the same diamond grain.

intersects the top {001} facet. SE images of such a grain viewed at three different specimen tilts are shown in Fig. 3. The {111} facets on the sides of the crystal appear rough compared to the (001) facet. The fracture surface is not perfectly planar but has many steps, as indicated with arrowheads in Figs. 3(a)–3(c). The original surface of the {111} facet was removed by the fracture, and steps were seen, corresponding to those arrowed in Fig. 3(a). Figure 3(d) illustrates the geometry of this diamond grain corresponding to the perspective of Fig. 3(a) and shows the three {111} facets, the top (001) facet (toward the observer), and the steps on the fracture surface (indicated by dashed lines).

The combination of SE and TEM images is a powerful advantage in our method for localizing defect structures in diamond films. The diamond grain shown in Fig. 3 was examined with TEM, first with a beam direction of [112]. The transmission of electrons would have been prevented by the specimen thickness if the $(\bar{1}\bar{1}1)$ facet had not been removed by the fracture since it would have been edge-on. The 3-D surface morphology of the grain at [112] can be directly visualized and identified in the SE image [Fig. 4(a)]. In the bright field (BF) TEM image [Fig. 4(b)], the grain exhibits two different types of contrast: a uniform contrast region (A) consisting of several steps produced from the fracture and the region with rough contrast (B) located at both sides of the grain. Selected area diffraction (SAD) from the uniform contrast region (A) indicates a perfect diamond structure. However, SAD from the rough contrast region (B) shows the extra reflections associated with the formation of microtwins. The region exhibiting uniform contrast in the BF image is free of microtwins.

To locate the distribution of microtwins, a dark-field image of this grain is shown in Fig. 4(c). The long exposure time of this image allowed features in the thick regions to be revealed. The most important feature of Fig. 4(c) is that two regions of distinctly different contrast are formed on the projected image of the same (111) facet, separated by the lines indicated by arrowheads in Fig. 4(c). Their position is inconsistent with the external shape of the grain [see Fig. 4(d)]. Figures 4(c) and 4(d) indicate that the microtwins are distributed not only on the {111} faces but are also found

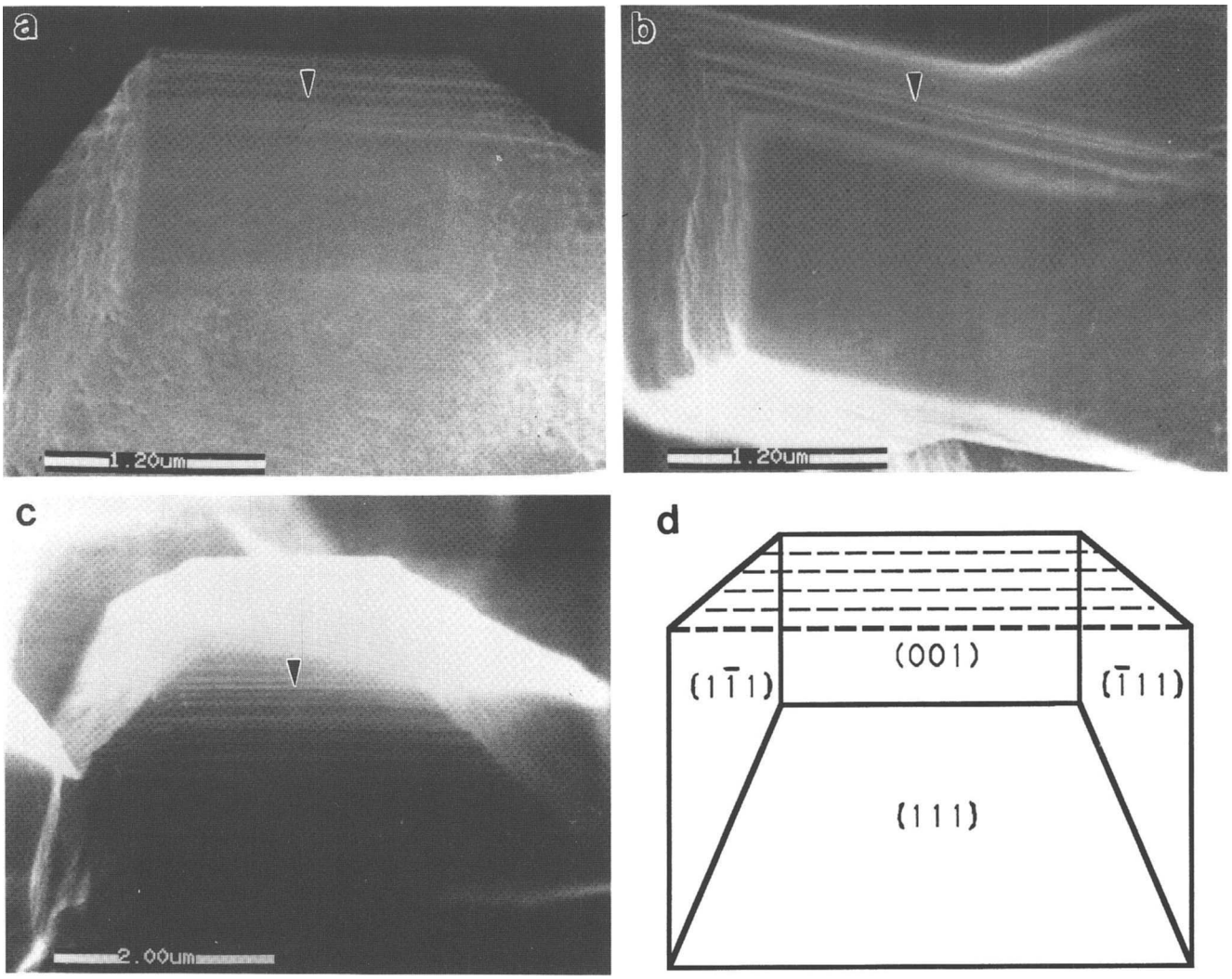

FIG. 3. SE images of a fractured diamond grain with fracture surface intersecting (001) top as seen from (a) the film side, (b) the grain top, and (c) the fractured surface side. Part (d) is a schematic drawing of the grain geometry, the fractured surface being indicated by dashed lines and located on the backside.

in parts of the grain interior. Well-defined boundaries on {110} separate the volume containing the microtwins from a central core volume underneath the {001} facet that is free of microtwins.

In order to confirm this interpretation, the crystal was tilted to a [101] beam direction. In this case, as shown schematically in Fig. 5, the contrast within the (001) projected area would be uniform without any sharp change if the microtwins were distributed merely on the {111} surfaces. Figure 6 shows the corresponding experimental observations from the same grain as in Fig. 4. The microtwins associated with the (1$\bar{1}$1) facet can be clearly identified by the SAD patterns shown in Fig. 6(a). Steps introduced by the fracture and the roughness of the {111} facets seen in Fig. 3(a) can be distinguished in the TEM images. The grain edges can be seen in the DF image taken with a matrix reflection [Fig. 6(b)]. Contrary to the schematic shown in Fig. 5, contrast regions separated by sharp lines (indicated with arrrowheads) are present in Fig. 6(b). Similar contrast character also appears in the DF image formed with a twin reflection [Fig. 6(c)], although diffuse scattering is responsible for the contrast in the thicker regions. The observations indicate that the volume filled with microtwins is bounded by internal (110) and ($\bar{1}$10) and the external {111} facets. Only the volume directly underneath the (001) facet is free of microtwins. The twin-planes are {111}. The bright line contrast in Fig. 6(c) at the ($\bar{1}$11) edge-on facet indicates the presence of microtwins, but no microtwins appear below the (001) surface. This is again an indication that growth on the {111} facets is responsible for the formation of microtwins. As the {001} facet grows, a microtwin-free column is produced below it.

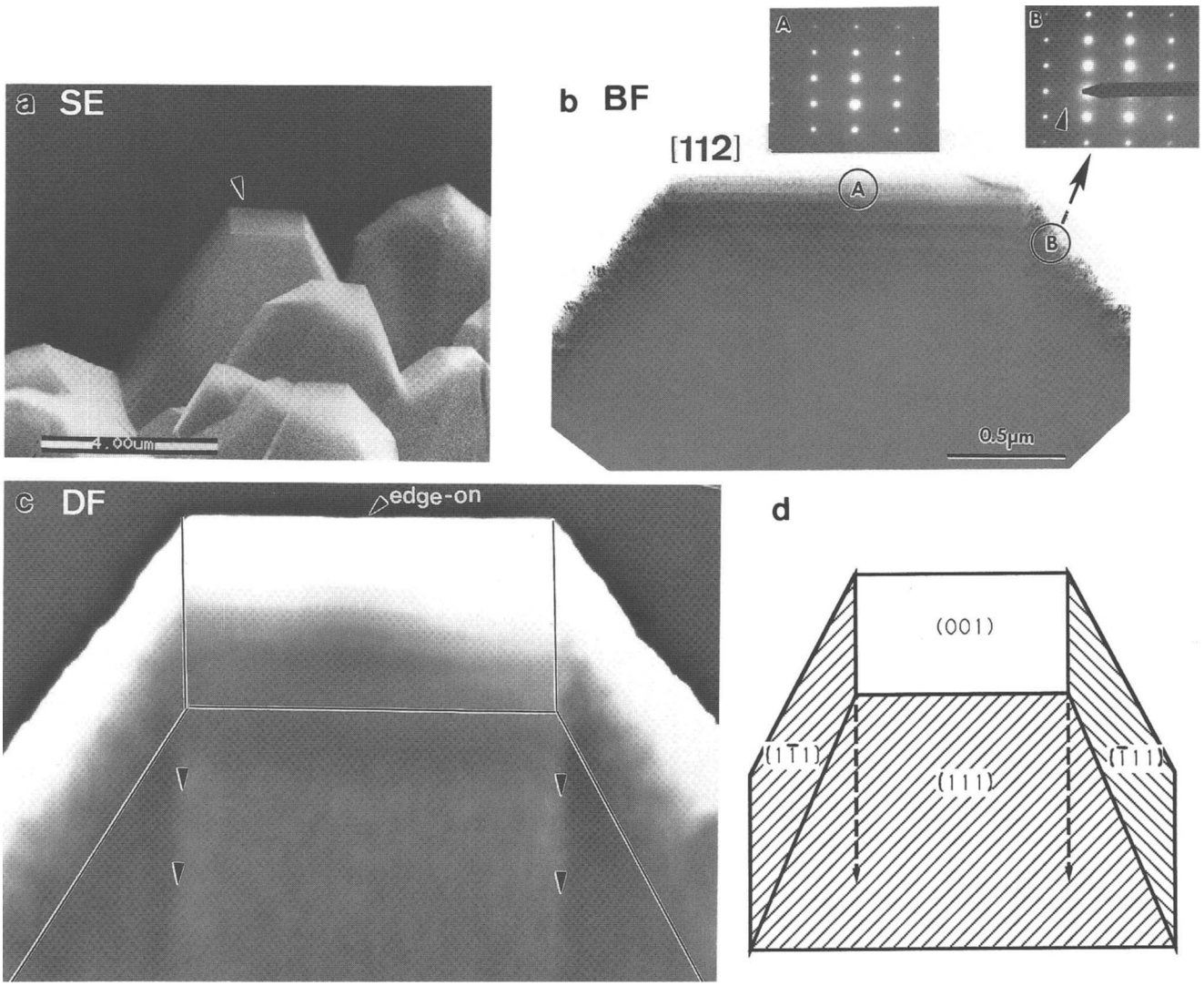

FIG. 4. (a) A SE image and the corresponding (b) BF and (c) DF images of the diamond grain shown in Fig. 3 viewing in the [112] direction. The insets are SAD patterns from the different regions. Part (d) is a geometrical model to illustrate the contrast effects appearing in the BF image. The presence of the microtwins can be directly seen.

B. Grains with fractures intersecting only {111} facets

The experimental studies described in the last section were for a diamond grain fractured so that microtwins associated with one of the {111} facets were removed completely. They showed that the microtwins were distributed within a certain volume of the grain, leaving a core volume free of microtwins. This structural model can be confirmed by the following additional experimental observations. For a diamond grain with a fracture surface that intersects only {111} facets, the volume under the remaining part of the fractured {111} facet should contain microtwins. This case is shown in Fig. 7. The diamond grain has essentially the same geometry as the grain examined in Figs. 3–6 except that a part of the fractured $(\bar{1}\bar{1}1)$ facet, indicated by arrow 1, remains. The (001) top facet and rough surface left by the fracture can be clearly identified in the SE image (Fig. 7).

The TEM examination of this diamond grain is shown in Fig. 8. The SAD pattern from area 1 shows the presence of microtwins of the same character as those observed in Fig. 6. The area with nonuniform contrast was observed at area 1 [Figs. 8(a) and 8(b)], corresponding to the projection of the unfractured volume filled with microtwins. In the [101] orientation, the $(\bar{1}11)$ plane intersecting with the fracture surface is projected edge-on, so that the microtwins would appear as a line in the image if they were distributed only on the {111} surface of the facet. However, the contrast effect shown at area 1 clearly indicates that the small volume left by the fracture is filled with microtwins. This evidence supports the observations presented in the last section. The contrast line produced by the edge of the microtwin

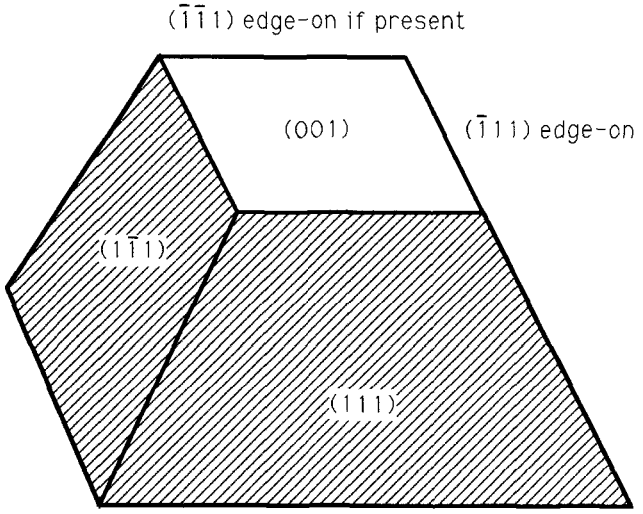

FIG. 5. A schematic model of contrast distribution in a BF TEM image of the diamond grain shown in Fig. 4 viewing in the [101] direction, assuming the microtwins are distributed only on the {111} facet surfaces.

distribution within the grain can be identified (indicated by the arrowhead at 2) and is similar to that observed in the last section.

C. Fractured grains with no (001) facet

Experimental observations in the last two sections have shown that transgranular fracture is a key feature which allows us to locate the microtwin distribution exactly. For an unfractured diamond grain, it would be impossible to locate the microtwin distribution inside the volume if the {111} facets are covered with microtwins. Figure 9 shows SE images of a fractured tetrahedral diamond grain with four {111} facets. This grain is a part of the same film that was discussed in the previous sections though it had only {111} facets on the surface. The TEM examination of this grain is shown in Fig. 10. In the [101] orientation, at the two edge-on {111} facets the specimen is too thick to allow clear TEM imaging, but the BF image from a thin corner shows microtwins on {111} [Fig. 10(a)]. Steps of height about 5–10 nm (arrowed) can be seen at the edge-on ($\bar{1}\bar{1}1$) surface. In the [001] orientation, DF images [Fig. 10(d)] formed with a twin reflection show microtwins associated with each {111} facet, but it is difficult to distinguish whether the microtwins are inside the bulk or on the surface. In the [112] orientation, for which one of the ($\bar{1}\bar{1}1$) facets is edge-on and exhibits 5–10 nm high surface steps (Fig. 11), the microtwins associated with two other {111} facets were identified by SAD, the twin-reflection DF image clearly indicating that the whole grain contained microtwins. There was no orientation along which the diamond grain showed a microtwin-free volume.

Although the microtwin structure readily forms on {111} facets, it is a thermodynamically unstable state. *In situ* TEM experiments have indicated, however, that the microtwin structure in a diamond film is preserved even when following heating to about 1230 °C. Our results from *in situ* annealing experiments have shown that the distribution of defects is almost unchanged after heating.[8] These results are at variance with the observation of Narayan who observed the presence of twin-free regions after rapid thermal annealing for 5–30 s at 1000 °C.[4]

D. TEM observations of the film-substrate interface

TEM examination of as-fractured films can also be applied to image the microstructure of diamond films at the substrate interface. It was found that an as-grown diamond film could be easily removed from the silicon substrate by cleavage, and that following tilting of the TEM specimen holder as shown in Fig. 12(a), the initial growth face could be examined. Figure 12(b) shows the microstructure of the diamond film at the substrate. The grains are much smaller than those located on the top growth face and there seems no specific orientation relationship among the grains. This is probably because the initial nucleation of each grain is an independent event. Microtwinned regions can be identified [see arrowed part in Fig. 12(b)].

Fracture can also produce some familiar shapes of micro-size "tools", as shown in Fig. 13. The diamond "drill" [Fig. 13(a)] was formed in a diamond fracture from an edge formed by two {111} facets and is filled with microtwins. The "saw" [Fig. 13(b)] was fractured from a {001} microtwin-free volume and shows thickness fringes. The saw teeth are extremely sharp.

IV. A MODEL FOR MICROTWIN DISTRIBUTION IN DIAMOND FILM

As a summary of the experimental observations in Sec. III, a defect structural model, which describes the microtwin distribution in CVD-grown diamond grains, is described. The core volume defined by the (001) top facet and its projection along the [001] growth direction with boundaries defined by orthogonal {110} internal planes (i.e., the volume enclosed by the dashed lines in Fig. 14) was free from microtwins. The remaining grain volume around the core, bounded by {111} facets and the {110} internal planes, was filled with microtwins. This will be referred to as the microtwin-free column model. The length of the column is determined by the crystal growth process (see Sec. VI). The formation of microtwins in CVD diamond is clearly associated with the growth of {111} facets. The results reveal a growth

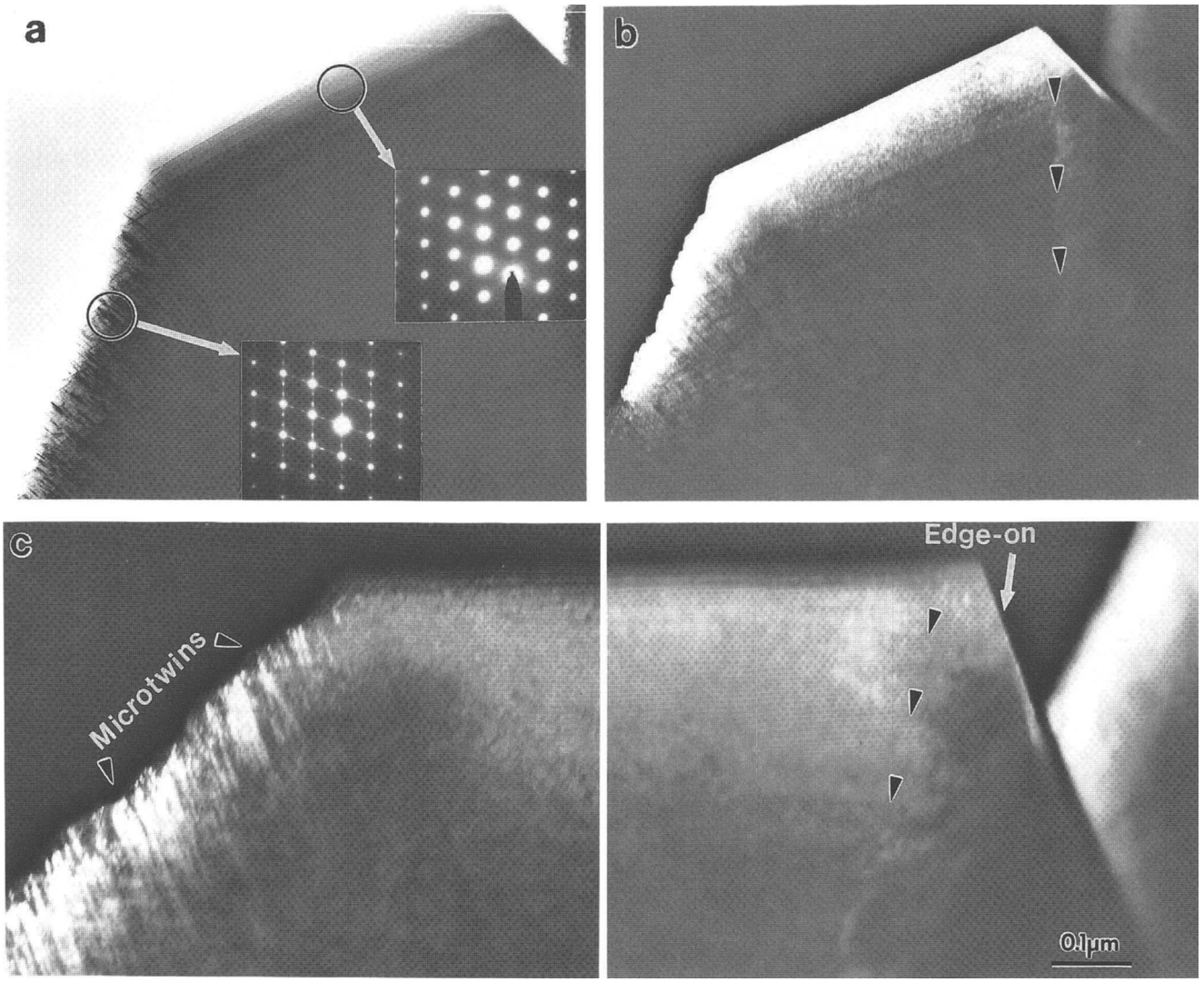

FIG. 6. (a) BF, (b) DF matrix reflection, and (c) DF twin reflection $1/3(11\bar{1})$ images of the diamond grain shown in Fig. 4. The beam direction is [101]. The insets are SAD patterns from different regions. The arrowed contrast line indicates the presence of microtwins inside the grain.

mechanism in which microtwins are formed as material is added to {111} but not {001} planes[5] and directly confirm this growth mechanism previously suggested by several authors.[2,6,7]

V. TEM OBSERVATIONS OF SECTIONED (ION-MILLED) FILMS

The boundaries on {110} between the microtwin-free core and the surrounding microtwinned regions cannot be easily studied at high resolution using the technique introduced above because the specimen was fractured along the [001] growth direction, resulting in a large thickness parallel to the boundary plane. This limitation may be overcome by the use of a conventional thinned TEM specimen. In addition, the experimental observation of a thinned diamond film would provide a useful check for consistency of the proposed defect model.

For these reasons, a plan-view diamond film was back-thinned from the substrate and ion-milled from both sides following the more traditional TEM specimen preparation procedures; thus, the images obtained from this plan-view specimen would give the microtwin distribution at a certain depth of the film. The specimen normal is the growth direction which has a strong [001] texture. Figure 15(a) shows a low magnification TEM image of a thinned plan-view specimen. Each square in the image represents the section through a microtwin-free core of a diamond grain surrounded by the microtwinned regions in dark contrast. The SAD patterns from the two different regions show patterns consistent with the previous observations. The microtwins would not appear in these images if they were distributed merely on the {111} facets. The boundary of the square-shaped microtwin-free core is jagged rather than being a smooth well-defined interface. The corresponding DF image

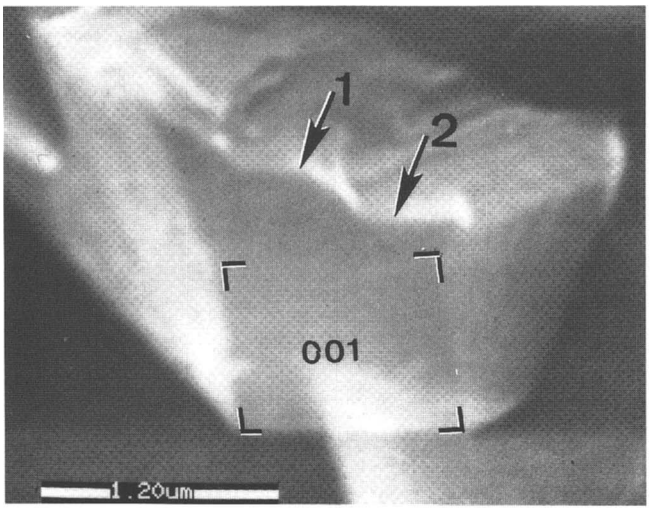

FIG. 7. SE image of a diamond grain with the fracture surface intersecting {111} facets only. The volume indicated by arrowhead 1 is unfractured.

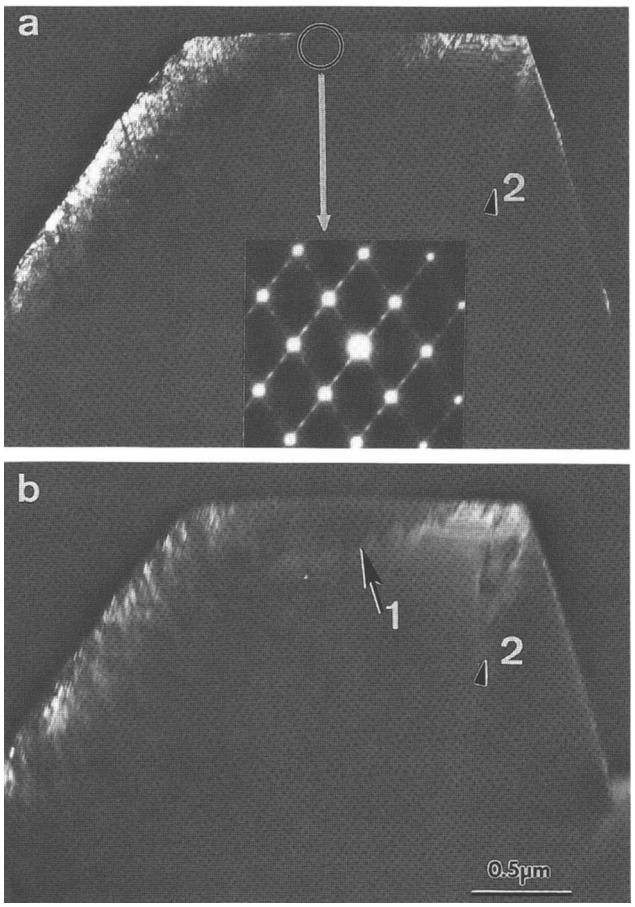

FIG. 8. DF twin reflection TEM images of the diamond grain shown in Fig. 7 viewing in the [101] direction. The inset is a SAD pattern from the region indicated by arrow 1, showing the presence of microtwins in the unfractured region. The area with nonuniform contrast was observed at area 1 (a, b).

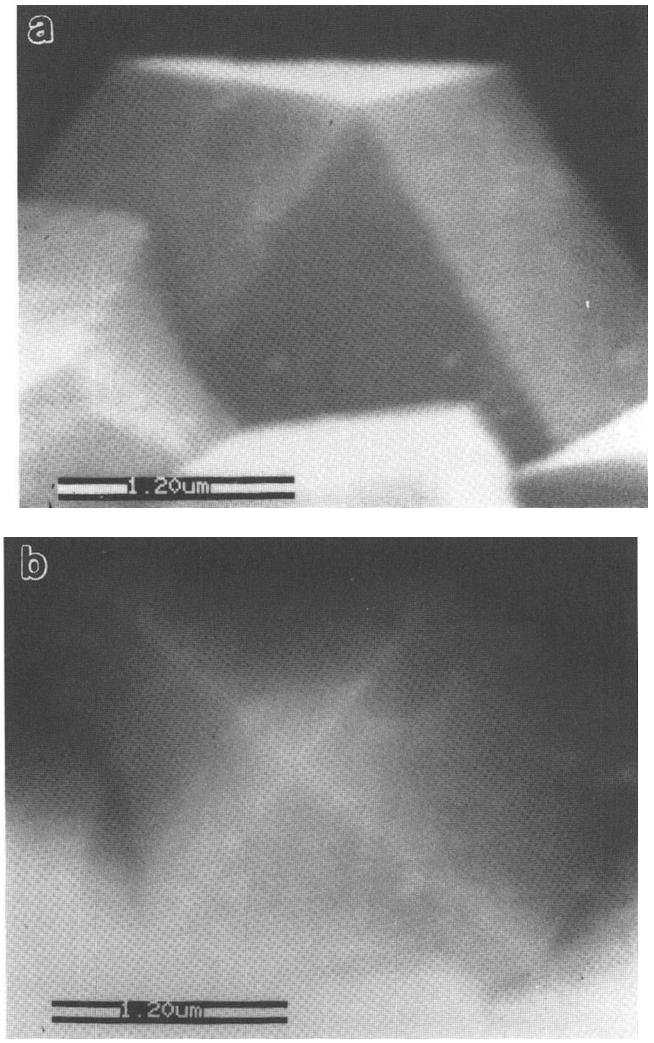

FIG. 9. SE images of an unfractured diamond grain as seen from (a) the film side and (b) the grain top.

using a matrix diffraction reflection shows that the two distinct regions belong to the same grain [Fig. 15(c)]. In other words, the microtwins are grown on the perfect diamond grain following specific orientation and they are not artifacts produced during specimen preparation. The DF image using a twin reflection verifies this statement [Fig. 15(d)]. In addition, the size of the (001) twin-free column is consistent with that shown in Fig. 4 which was obtained from a fracture specimen. Thus, the observations shown in Fig. 15 clearly support the microtwin-free column model.

As a further check, the diamond grain shown in Fig. 15 was tilted to the [101] orientation. In agreement with the observations at [001], the twin reflections appear only in the SAD patterns from the regions of dark contrast surrounding the core [Fig. 16(a)]. The DF image formed with a twin reflection shows the distribution of microtwins around the {001} column [Fig. 16(b)].

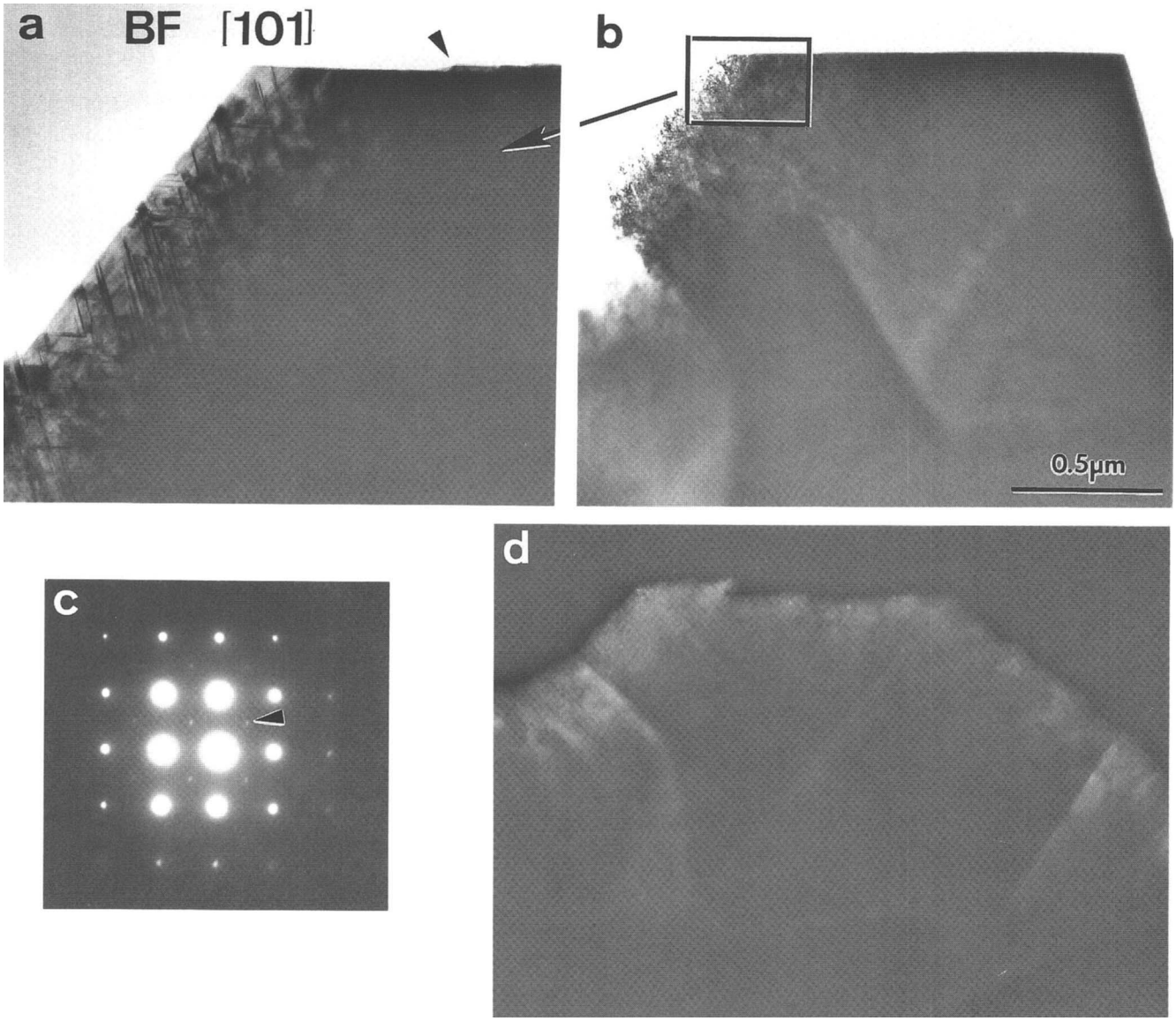

FIG. 10. (a) and (b) are BF TEM images of the diamond grain shown in Fig. 9 viewing along [101]. Part (c) is a [001] SAD pattern of the same grain showing the presence of twin reflections. Part (d) is a DF twin reflection [indicated in (c)] TEM image of the grain viewing in the [001] direction, showing that the grain is filled with microtwins.

VI. DISCUSSION

Studies of defect distributions in CVD diamond films using conventional TEM methods have been reported by several authors. They seem to agree that the formation of microtwins and stacking faults is related to growth on {111}, but no direct, definitive evidence has been presented and there have been few conclusions concerning the distribution of microtwins. Zhu *et al.*[9] showed that the microtwins and stacking faults lie on {111} in diamond film, but were unable to determine the microtwin distribution. They suggested that the formation of these structural imperfections may be one of the main obstacles to developing tailored structures and properties for particular applications of diamond films. Investigations of Kaae *et al.*[10] and Hetherington *et al.*[11] have suggested that the defects are eliminated from the center of the crystal and occur only at grain boundaries where the growing crystallites meet. Their results seem to suggest that the formation of microtwins is a direct effect of grain boundaries. The observations by Badzian *et al.*[12] have also shown the high perfection of the ⟨001⟩ sector and the high density of planar defects in the ⟨111⟩ sector. The microtwin-free column model (Fig. 14) explains these observations, whereas the models proposed by the authors are less specific and less complete.

In work particularly relevant to our observations, Stuart *et al.*[13] have grown diamond particles (or grains) on fine tungsten wire tips to study the early stages of crystal growth. This allowed them to examine single diamond particles with TEM techniques without spec-

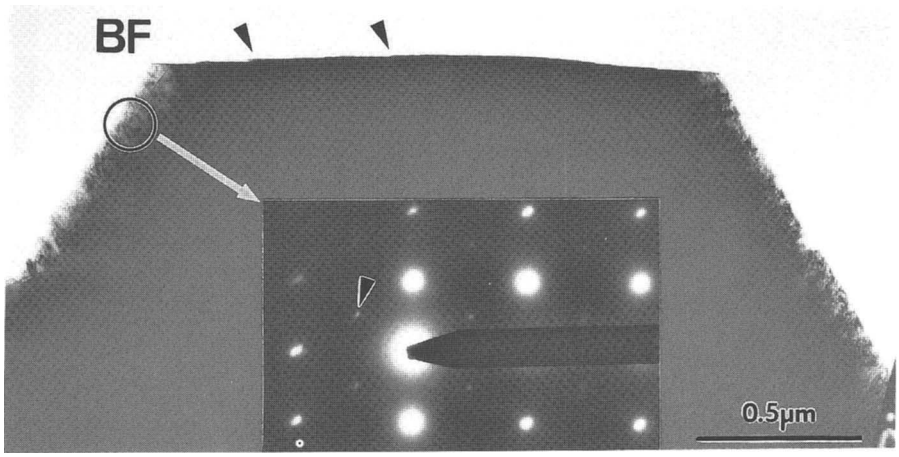

FIG. 11. BF TEM image of the diamond grain shown in Fig. 9 in the [112] orientation. The inset is the SAD pattern.

imen preparation and to correlate the results with SEM and Raman spectroscopy of the same particles. Their results indicate that the (001) faces are better quality diamond than the (111) faces, and support the proposal of Hetherington *et al.*[11] that the growth of the {001} and {111} faces are, respectively, driven by epitaxial and secondary nucleation of 1 nm high diamond islands on the surface. Significantly, micro-Raman spectra were recorded from different positions on individual grains. An intense phonon peak located at 1333 cm^{-1} was clearly resolved in spectra from {001} and {111} facets, indicating that the material of both facets is close to perfect diamond. The presence of a broad feature in the range 1500–1550 cm^{-1} indicated a more disordered structure from the {111} facets. Through the studies in this paper, the broad Raman peaks can be attributed to the phonon states in the region containing microtwins associated with {111} facets. The model of Stuart *et al.*'s[13] method may provide an effective way for studying the properties of each diamond grain at an early stage before film formation, but may not be readily applied to fully characterize the defect distribution inside the grain.

The morphology of diamond films is determined by the growth rates of various faces.[7] On (001) planes attachment of single-carbon-atom species is energeti-

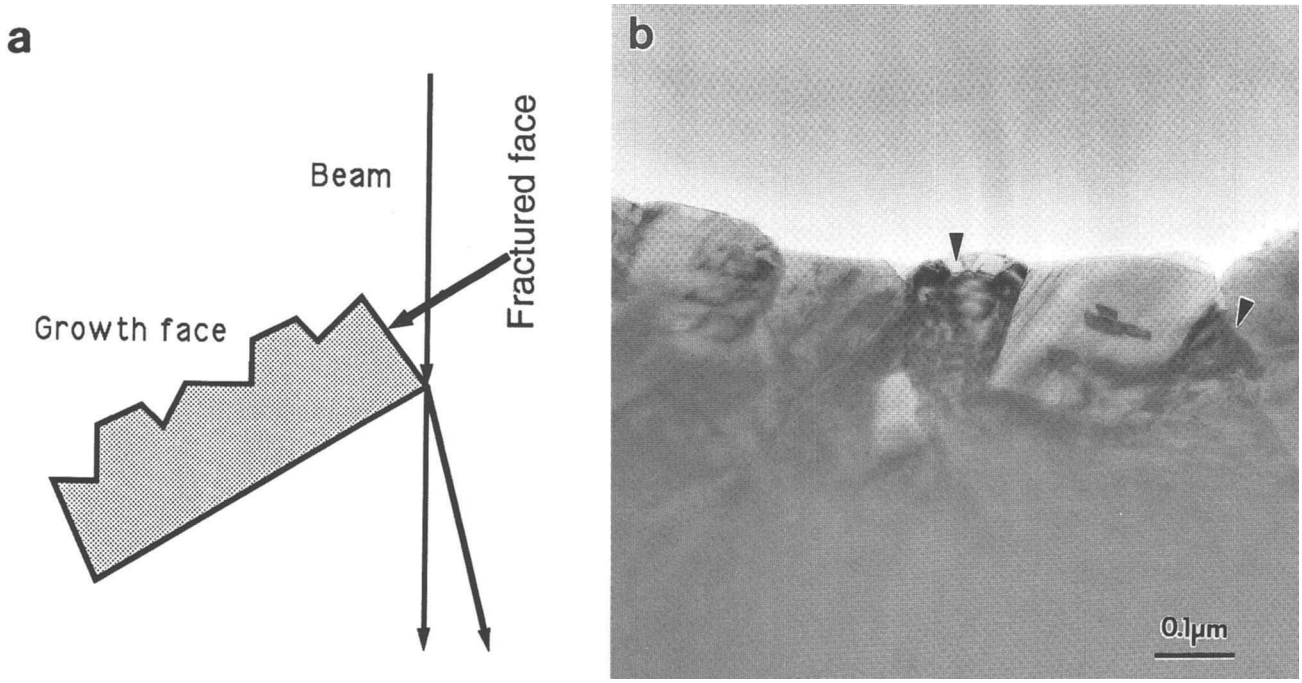

FIG. 12. (a) A schematic model for imaging the initial nucleation of an as-grown diamond film with the technique introduced in this paper. (b) A BF TEM image of the initial growth face. The grain sizes are much smaller than those shown in Fig. 2(c).

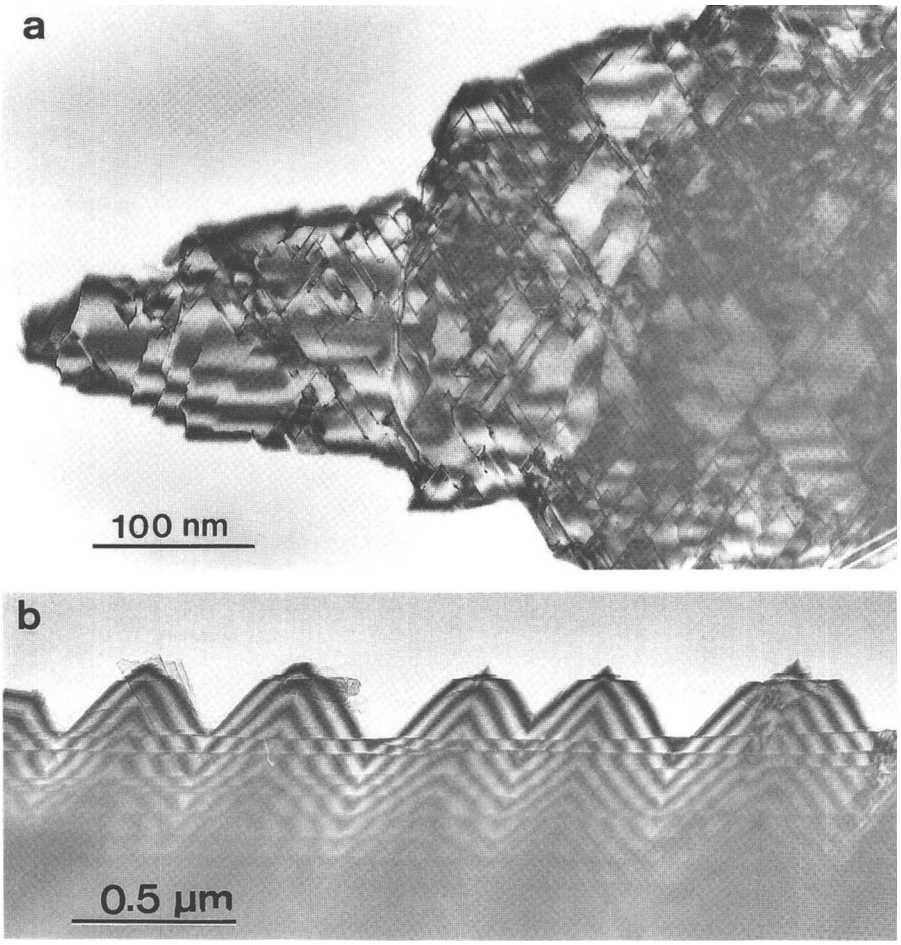

FIG. 13. "Drill" (a) and "saw"-shaped (b) micro-size diamond pieces produced in film fracture.

cally favored because they can make two bonds with the surface. Furthermore, addition of carbon atoms to these two-bonded identical sites automatically extends the diamond-cubic lattice. This is the reason that no microtwins develop on (001) facets. On the other hand, the relatively strain-free nuclei on {111} surface are a three-membered bridge and a four-membered nucleus.[6,14] Two-carbon-atom species can be added in two different configurations, giving the possibility of creating microtwins.

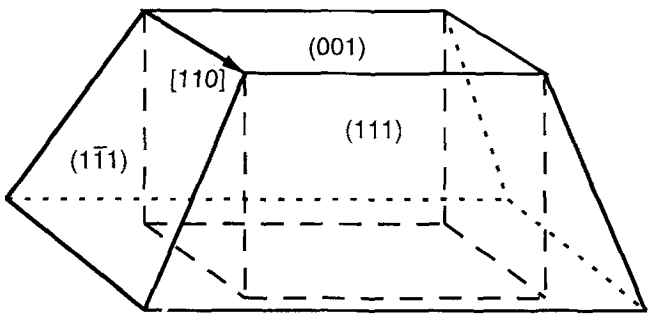

FIG. 14. A microtwin-free column model. The core volume enclosed by the dashed lines is free from microtwins; the remaining volume is filled with microtwins. The dotted line indicates the back side of the diamond grain.

Angus and Hayman[6] have argued that crystals with {001} faces are formed when atoms are rapidly added to {111} planes and that crystals with {111} faces are formed when atoms are rapidly added to {001} planes. The presence of both {001} and {111} faces in our experiments indicates that the growth rates of the two faces are not vastly different. The computer simulation of Clausing *et al.*[7] indicates that for the diamond film used in this study the growth rate on ⟨001⟩ is 1.0–1.15 times that along ⟨111⟩.

The initial grains in the present films appeared to be oriented randomly. The transition to a highly textured film presumably occurs by the competitive growth model of Van der Drift.[15] In this model, which has been used by Wild *et al.*[16] in computer simulations of diamond film growth, grains oriented with a rapid growth direction normal to the substrate will survive, and others will be gradually buried. Two other consequences of this process are the development of a preferential orientation and continual increase in grain size. In the diamond films studied here, we expect that the cross-

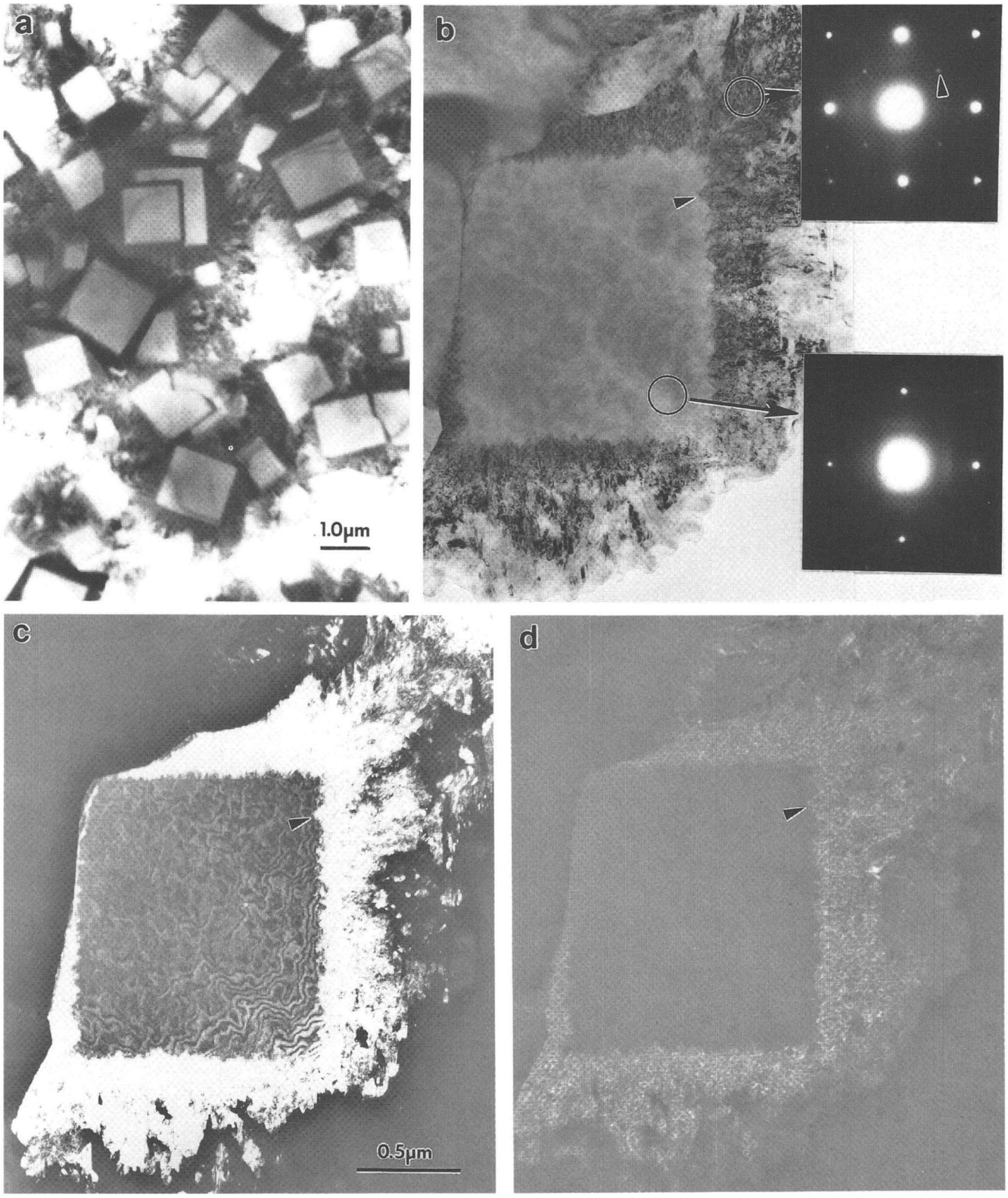

FIG. 15. (a) Low magnification, (b) BF, (c) DF matrix reflection, and (d) DF twin reflection TEM images of a conventional thinned plane-view diamond film viewed along the [001] direction showing the distribution of microtwins. The insets are SAD patterns. It is very difficult to distinguish from these images whether the microtwins are distributed merely on the {111} facets or inside the volume according to the model shown in Fig. 14.

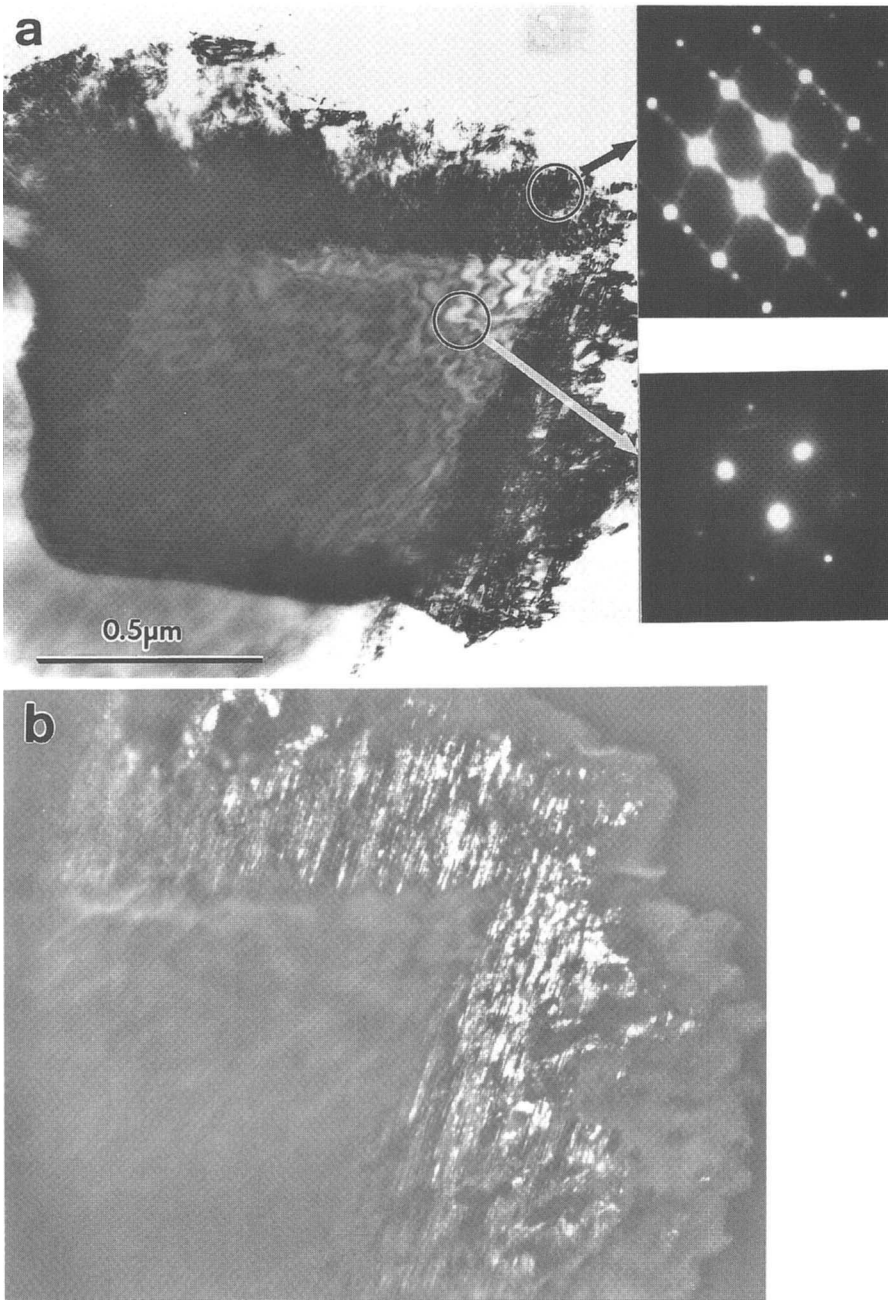

FIG. 16. (a) BF and (b) DF twin reflection images of the same grain shown in Fig. 15 viewed along the [101] direction. The insets are the SAD patterns.

sectional area of the microtwin-free column changes only very gradually. This suggestion is supported by the micrographs of the plan-view ion-milled TEM specimens where the defect-free cores are similar in size to those at the growth surface. Conventionally, thinned cross-section TEM specimens or plan-view specimens from different depths could provide detailed microstructural information to help understand how the cores form and develop.

According to the growth model presented above, a textured diamond film formed without {111} facets may not contain microtwins. To verify this statement, we have studied a film with a ⟨001⟩ texture but only with {001} facets.[5] The grains have cubic shapes, and TEM examination has shown that they are free from microtwins. Microtwins were not even observed near or at grain boundaries. This microstructure is greatly different from that of the diamond films studied in this paper and is highly relevant in understanding the formation of microtwin-free, cubic-shaped diamond grains. The results serve to further confirm our microtwin-free column model as shown in Fig. 13.

Recent applications of the technique introduced here to the studies of a diamond film of approximately 50 μm thickness grown at 1100–1120 °C in a mixture of H_2 and CH_4 have shown that the presence of twin boundaries allows {111} surface facets to exist and microtwinned material to grow in the midst of other material growing without microtwins from {001} facets. The growth of microtwinned regions complicates the surface morphology.[17]

VII. SUMMARY

A simple technique is introduced for studying films grown by CVD. For the first time, a thick as-grown diamond film was examined directly by conventional transmission electron microscopy without thinning, and the important microstructures near the growth surface were characterized. This new technique not only avoids tedious TEM specimen preparation, but also provides structural information that relates extended crystal lattice defects (dislocations and microtwins) to specific growth facets.

The formation of microtwins in CVD diamond is mostly associated with growth on {111}. Detailed observations were made on a diamond film with an ⟨001⟩ texture and having 2–3 μm-diameter grains with {001} top facets and four inclined {111} facets. After studying grains with fracture surfaces that intersected the top (001) facet, grains with fractures that intersected only {111} facets, and with only {111} faceted grains, we have found that the core volume bounded by the (001) top facet and orthogonal {110} is free from microtwins. The remaining volume around the core, bounded by {111} facets on the growth surface and extending to the grain boundaries, is filled with microtwins. The microtwins were not merely at the {111} surfaces. This microtwin-free column model comprehensively accounts for observations by several authors on the microtwin distributions in the diamond films. In addition, surface steps at least 5–10 nm high have been observed on {111} facets. Steps near atom-high on (001) facets have been observed with reflection electron microscopy.[18] Examination of conventionally thinned TEM specimens confirmed the above defect structural model.

Our results reveal a growth mechanism in which microtwins are formed as material is added to {111} but not {001} planes. The surface morphology and texture of diamond films are determined by the growth rates of different crystallographic faces and develops as the result of competition between grains oriented in different orientations (i.e., the Van der Drift model).

ACKNOWLEDGMENTS

We thank Dr. E. A. Kenik, Dr. J. M. Vitek, and Dr. R. Jayarama for comments. This research was sponsored by the Division of Materials Sciences, United States Department of Energy, under Contract DE-AC05-84OR21400 with Martin Marietta Energy Systems, Inc.

REFERENCES

1. G-H. M. Ma, Y. H. Lee, and J. T. Glass, J. Mater. Res. **5**, 2367 (1990).
2. R. E. Clausing, L. Heatherly, and K. L. More, Surf. Coating Technol. **39/40**, 199 (1990).
3. B. E. Williams and J. T. Glass, J. Mater. Res. **4**, 373 (1989).
4. J. Narayan, J. Mater. Res. **5**, 2414 (1990).
5. Z. L. Wang, J. Bentley, R. E. Clausing, L. Heatherly, and L. L. Horton, in Applications of Diamond Films and Related Materials, edited by Y. Tzeng, M. Yoshikawa, M. Murakawa, and A. Feldman (Elsevier, Amsterdam, 1991), p. 489.
6. J. C. Angus and C. Hayman, Science **241**, 913 (1988).
7. R. E. Clausing, L. Heatherly, E. D. Specht, and K. L. More, in *New Diamond Science and Technology*, edited by R. Messier, J. T. Glass, J. E. Butler, and R. Roy (Mater. Res. Soc. Symp. Int. Proc. **NDST-2**, Pittsburgh, PA, 1991), p. 575.
8. Z. L. Wang, R. E. Clausing, L. Heatherly, and L. L. Horton, unpublished.
9. W. Zhu, A. R. Badzian, and R. Messier, J. Mater. Res. **4**, 659 (1989).
10. J. L. Kaae, P. K. Gantzel, J. Chin, and W. P. West, J. Mater. Res. **5**, 1480 (1990).
11. A. V. Hetherington, C. J. H. Wort, and P. Southworth, J. Mater. Res. **5**, 1591 (1990).
12. A. R. Badzian, T. Badzian, X. H. Wang, and T. Hartnett, in *New Diamond Science and Technology*, edited by R. Messier, J. T. Glass, J. E. Butler, and R. Roy (Mater. Res. Soc. Symp. Int. Proc. **NDST-2**, Pittsburgh, PA, 1991) p. 549.
13. S. Stuart, S. Prawer, A. Hoffman, and A. Moodie, in *Evolution of Thin Film and Surface Microstructure*, edited by C. V. Thompson, J. Y. Tsao, and D. J. Srolovitz (Mater. Res. Soc. Symp. Proc. **202**, Pittsburgh, PA, 1991), p. 217.
14. D. Meakin, J. Stoemenos, P. Migliorato, and N. A. Economou, J. Appl. Phys. **61**, 5031 (1987).
15. A. Van der Drift, Philips Res. Rep. **22**, 267 (1967).
16. Ch. Wild, N. Herres, and P. Koidl, J. Appl. Phys. **68**, 973 (1990).
17. Z. L. Wang, L. L. Horton, R. E. Clausing, L. Heatherly, and J. Bentley, Proc. 50th Annual Meeting of Electron Microscopy Soc. America (Boston), edited by G. W. Bailey, J. Bentley, and J. A. Small (San Francisco Press, San Francisco, CA, 1992), p. 336.
18. Z. L. Wang, J. Bentley, R. E. Clausing, L. Heatherly, and L. L. Horton, Proc. 51st Annual Meeting of Microscopy Society of America (Boston), edited by G. W. Bailey and E. L. Rieder (San Francisco Press, San Francisco, CA, 1993), p. 1006.